

# Investigating Protein Adsorption via Spectroscopic Ellipsometry

**Maria F. Mora, Jennifer L. Wehmeyer, Ron Synowicki,  
and Carlos D. Garcia**

In this chapter, the basic concepts behind ellipsometry and spectroscopic ellipsometry are discussed along with some instrument details. Ellipsometry is an optical technique that measures changes in the reflectance and phase difference between the parallel ( $R_p$ ) and perpendicular ( $R_s$ ) components of a polarized light beam upon reflection from a surface. Aside from providing a simple, sensitive, and nondestructive way to analyze thin films, ellipsometry allows dynamic studies of film growth (thickness and optical constants) with a time resolution that is relevant to biomedical research. The present chapter intends to introduce ellipsometry as an emerging but highly promising technique, that is useful to elucidate the interactions of proteins with solid surfaces. In this regard, particular emphasis is placed on experimental details related to the development of biomedically relevant conjugated surfaces. Results from our group related to adsorption of proteins to nanostructured materials, as well as results published by other research groups, are discussed to illustrate the advantages and limitations of the technique.

## Abbreviations and Symbols

$\Gamma$	Adsorbed amount
$d\Gamma/dt$	Adsorption rate
$\Delta$	Phase difference
$\lambda$	Wavelength
$\psi$	Amplitude
AFM	Atomic force microscopy
BSA	Bovine serum albumin
CNT	Carbon nanotubes

---

**M.F. Mora and C.D. Garcia** • Department of Chemistry, The University of Texas at San Antonio, San Antonio, TX 78249 USA

**J.L. Wehmeyer** • Department of Biomedical Engineering, The University of Texas at San Antonio, San Antonio, TX 78249, USA

**R. Synowicki** • J. A. Woollam Co., Inc, 645 M Street, Suite 102, Lincoln, NE 68508, USA

$d$	Thickness
DAAO	D-amino acid oxidase
DC	Direct current
DNA	Deoxyribonucleic acid
EMA	Effective medium approximation
Fib	Fibrinogen
HSA	Human serum albumin
IEP	Isoelectric point
$k$	Extinction coefficient
$n$	Refractive index
$R_p$	Parallel component of polarized light beam
$R_s$	Perpendicular component of polarized light beam
SDS	Sodium dodecyl sulfate
SE	Spectroscopic ellipsometry
$t$	Time

## 2.1. Introduction

Interaction of proteins with material surfaces is a common but rather complicated phenomenon [1]. One of the most remarkable consequences of this interaction is that materials coated with biomolecules display the properties of the adsorbed protein layer, rather than the material itself [2]. Consequently, understanding the protein adsorption phenomena is critical for the rational design of biologically active composites with sensing, biological, and electronic functions.

Among other substrates, nanomaterials are part of an industrial revolution that provides materials with unique properties (thermal, mechanical, electrical, biological, etc.) not found in conventional/microphased materials [3–7]. The combination of remarkable recognition capabilities of biomolecules with the unique properties of nanomaterials resulted in systems with significantly improved performance [8]. Apart from mechanical strength and light weight, most of the extraordinary biological properties of nanomaterials are linked to unique surface properties (surface area, surface roughness, energetics, and altered electron distributions) [9], which enable improved interactions between material surfaces and biological entities. Most importantly, the type and conformation of proteins adsorbed to nanomaterials proved to be a key factor in subsequent cellular responses [4]. Consequently, various experimental parameters must be optimized in order to control the biological activity of the bio/nano composite. Proteins, which tend to spontaneously accumulate at interfaces with materials, may undergo structural changes upon adsorption. The extent of such conformational changes induced by the sorbent surface depends on the material surface properties, the protein, the pH, and the degree of protein coverage of the surface. Understanding these conformational changes is probably one of the most important points for biomedical applications because they can *generally* be controlled. In this respect, the structural stability of the protein, defined by differential scanning calorimetry as “soft” or “hard” proteins, can provide the first indications about the driving forces behind, and consequences of, protein–biomaterial interactions [10, 11]. Further details regarding the adsorption of proteins to biomaterials can be found in other chapters of this book.

From the kinetics standpoint, the rate of protein adsorption at the solid/liquid interface comprises two steps: (1) transport of the solute molecules toward the interface and

(2) interaction with the sorbent material surface. The basic mechanisms of transport of molecules to the material surface are diffusion and convection by either laminar or turbulent flow. In the second step, the adsorbate molecules may attach at, or detach from, the sorbent material surface, giving rise to two fluxes, one forward and one backward. The relative contributions of each one of these fluxes to the overall adsorption process depend on both the attraction exerted by the material surface to the adsorbate and the solvent–sorbent interactions. Many energetic and entropic effects contribute to the free energy of the protein adsorption process. However, when proteins are adsorbed at the solid/liquid interface, the main driving forces of the interaction are electrostatic and hydrophobic ones. In the simplest case, the protein adsorption rate ( $d\Gamma/dt$ ) may be considered as a first-order process, as described by Eq. (2.1):

$$\frac{d\Gamma}{dt} = k_{\text{ADS}} C_{\text{S}}, \quad (2.1)$$

where  $k_{\text{ADS}}$  is the adsorption rate constant and  $C_{\text{S}}$  is the concentration of solute (proteins, in the case under consideration). As the material surface coverage increases with time,  $k_{\text{ADS}}$  decreases, and an equilibrium is reached ( $\Gamma_{\text{SAT}}$ ). When changes in the structure of the protein upon adsorption occur, the process could be described by considering an equilibrium reaction, in which the protein in solution can interact with the material surface, adsorb, and subsequently, undergo a structural/conformational change on that material surface. Such equilibria have been described for diverse proteins including lysozyme [12], albumin, and fibrinogen [13–18].

Kinetic and thermodynamic studies have indicated that significant conformational changes may occur as a protein adsorbs to a surface [19]. For this reason, many different techniques have been used to study not only the adsorption/desorption phenomena but also structural changes of such interactions [20]. Among others, Brewster angle microscopy, neutron and X-ray reflection, fluorescence and time-resolved fluorescence, circular dichroism, infrared spectroscopy, and electron microscopy were discussed in a book edited by Baszkin and Norde [21]. Studies of protein adsorption using mass spectrometry [22], confocal laser scanning microscopy [23], neutron reflection [24], atomic force microscopy (AFM; see other pertinent chapters in this book), scanning force microscopy [25], optical waveguide light-mode spectroscopy [19], quartz crystal microbalance [26, 27], surface plasmon resonance, total internal reflection fluorescence [28, 29], and capillary electrophoresis [30–33] have been also reported in the scientific literature.

## 2.2. Ellipsometry

Another technique that can provide information regarding the protein adsorption processes as well as the structure of the adsorbed protein layer is ellipsometry. Ellipsometry is an optical technique that measures changes in the reflectance and phase difference between the parallel ( $R_{\text{p}}$ ) and perpendicular ( $R_{\text{s}}$ ) components of a polarized light beam upon reflection from a surface. Using Eq. (2.2),

$$\tan(\psi)e^{i\Delta} = \frac{R_{\text{p}}}{R_{\text{s}}}, \quad (2.2)$$

the intensity ratio of  $R_p$  and  $R_s$  can be related to the amplitude ( $\psi$ ) and the phase difference ( $\Delta$ ) between the two components [34]. Because ellipsometry measures the ratio of two values originated by the same signal, the data collected are highly accurate, and reproducible. Most importantly, no reference specimen is necessary. The changes in polarization measured by ellipsometry are extremely sensitive to film thickness (down to the monolayer level), optical constants, and film microstructure (such as surface roughness, index grading, and intermixing). This monolayer sensitivity is useful for real-time studies of layer-by-layer film deposition, including biological monolayers on a variety of substrates.

When substrates are flat, isotropic, and uniform, the interpretation of the ellipsometry results is relatively simple. Needless to say, biological substrates rarely meet these specifications, and often present multiple layers with different thicknesses, optical constants, and topographies. Because of the complexity of biological substrates, data must be obtained at multiple wavelengths and angles. Since the time of early applications, which were mainly focused on thickness quantification of oxide layers, ellipsometry has evolved to spectroscopic ellipsometry that is able to resolve details in the kinetics of layer formation for a variety of molecules [35] and even to investigate two-dimensional film thickness profiles with high spatial resolution and sensitivity [36–40]. Aside from providing a simple and nondestructive way to analyze thin, organic layers of biological interest, ellipsometry allows dynamic studies of film growth (thickness and optical constants) with a relevant time resolution.

### 2.3. Optical Models Used to Interpret Ellipsometric Results

Interpretation of ellipsometric measurements from raw data ( $\psi$  and  $\Delta$ ) is rather difficult and requires an optical model that describes the substrate microstructure in terms of refractive index ( $n$ ), extinction coefficient ( $k$ ), and thickness ( $d$ ). This requirement is probably one of the biggest limitations of the technique, because the reliability of the calculated properties is only as good as the model used [41]. A second limitation (pertaining mostly to very thin films substrates), is that ellipsometry is not very sensitive to the value of  $n$ , because the  $n$  and  $d$  values of very thin films are highly correlated [42]. On the other hand, advances in instrumentation, matrix multiplication procedures, and modern computer applications enable modeling ellipsometric data with multilayer structures with better accuracy, reasonable time, and different optical models [43]. Most modern instruments provide comprehensive software packages with a built-in mean square error calculation that can be used to quantify the difference between the experimental and model-generated data.

The main objective of ellipsometry data analysis is to achieve an accurate description of the substrate using the simplest possible model. The procedure employed generally includes several iterations through four main steps: (1) modeling the dielectric function, (2) constructing an optical model that describes the overall behavior of the system, (3) fitting the collected spectra to the optical model, and (4) calculating the fitting error. If done correctly, this procedure also minimizes the uncertainty associated with the measurements. In other words, the conclusions obtained by ellipsometry are only as good as the optical model.

Depending on the electronic properties of the materials tested, different optical models can be applied to the data collected by ellipsometry [34, 44]. In the simplest case, when the layers can be considered transparent and homogeneous, the refractive index ( $n$ ) as a function of the wavelength ( $\lambda$ ) can be described using a classical Cauchy model (Eq. 2.3):

$$n_{(\lambda)} = A + \frac{B}{\lambda^2} + \frac{C}{\lambda^4}, \quad (2.3)$$

where  $A$ ,  $B$ , and  $C$  are constants fitted by the model. Cauchy models have been used to study the structure of layers of biotin–avidin [45], albumin [46], ferritin [47], and polymers [48, 49], as well as binding of T-2 molecules to antibodies [50], and other small molecules [51, 52]. The interpretation of data related to biological molecules that absorb light (e.g., resonant electrons at 280 nm) requires the use of other models such as the Tauc–Lorentz model, which accounts for the unique band-gap of such amorphous materials. Tauc–Lorentz models have been used to describe the hemocompatibility of carbon thin films and their interaction mechanism with blood plasma proteins such as human serum albumin (HSA) and fibrinogen [53–57]. Similar models have also been used to evaluate the thrombogenicity of polysaccharide-coated surfaces [58].

These mathematical models used to describe each layer must be combined in a reasonable optical model that describes the overall behavior of the system. In this regard, most biomedically relevant substrates can be modeled by a small number of uniaxial layers with optical axes parallel to the normal axes of the substrate. Although other examples of these models abound in the literature, Figures 2.1 and 2.2 show two optical models used to describe biomedically relevant processes.

In the first case (*see* Figure 2.1), the model consists of a two-layer substrate (bulk silicon coated with a layer of amorphous hydrogenated carbon) and a protein layer (fibrinogen) as an overlayer [53]. An additional layer (four layers in total) was used to model the adsorption of  $\beta$ -casein at air/water and oil/water interfaces [60]. In situations where the

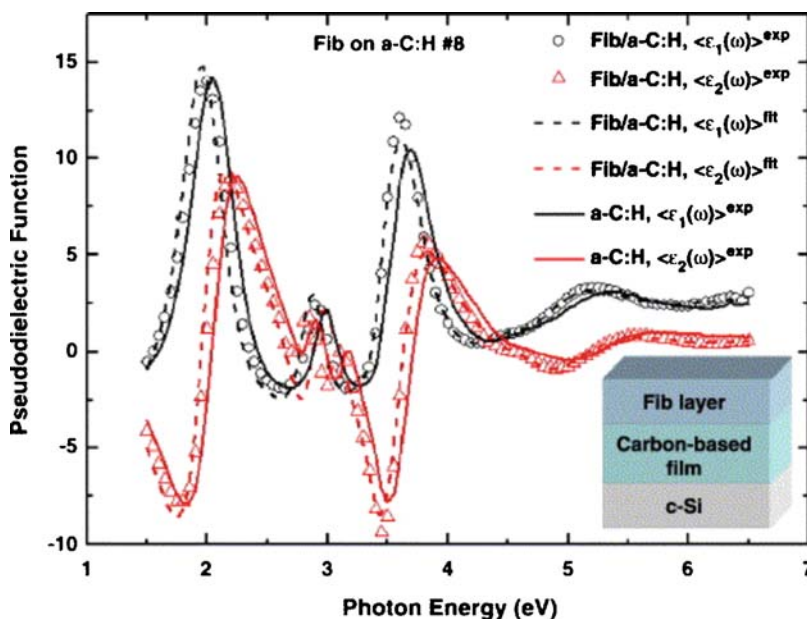


**Figure 2.1.** Three-layer model used to investigate the adsorption of fibrinogen (Fib) on hydrogenated carbon films. Reprinted from Ref. [53].

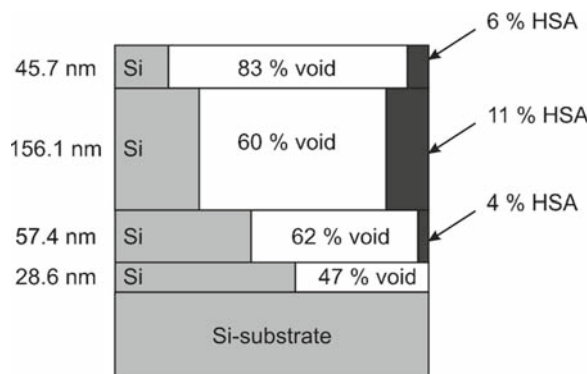


**Figure 2.2.** Five-layer model used to investigate the adsorption/penetration of human serum albumin (HSA) to porous silicon substrates. Reprinted from Ref. [59].

material surface and interface microstructures have to be accounted for, an effective medium approximation (EMA) model can be applied. EMA layers mix the optical constants of two or more materials and are extremely useful in modeling surface roughness [61], interface layers, and volume fractions in composite materials [62]. This is the case of the model illustrated in Figure 2.2, where a five-layer model, each layer with different composition (of silicon, void space, and protein), was used to investigate the adsorption of HSA to a porous silicon substrate [59]. Similar models were later used by Karlsson [46, 63] and Tsargorodskaya [64] to rationalize information related to the adsorbed protein amount as well as the concentration profile into the porous substrate. EMA layers also allow mixing materials, independently described by different optical models such as the Cauchy, Lorentz, or Tauc–Lorentz. EMA layers have been also applied to describe interactions between ferritin and gold [47].

Once the construction of an accurate optical model, describing the adsorbed protein layer (and the substrate), has been achieved, the thickness of a protein layer obtained by ellipsometry can be used to calculate the adsorbed protein amount ( $\Gamma$ , expressed in milligrams per meter squared) using Eq. 2.4:

$$\Gamma = \frac{d(n - n_0)}{(dn/dc)}, \quad (2.4)$$

where  $n$  and  $n_0$  are the refractive indices of the protein and the ambient environment, respectively [65]. In accordance with previous reports, the refractive index increment for the molecules in the layer ( $dn/dc$ ) is generally assumed to be around 0.187 mL/g [66–69].

## 2.4. Instrument Considerations

In general, ellipsometers are relatively simple instruments. Figure 2.3 shows schematically (and not to scale) the main components of a rotating analyzer spectroscopic ellipsometer. Light from a Xe–arc lamp is directed through a monochromator (1), collimated,

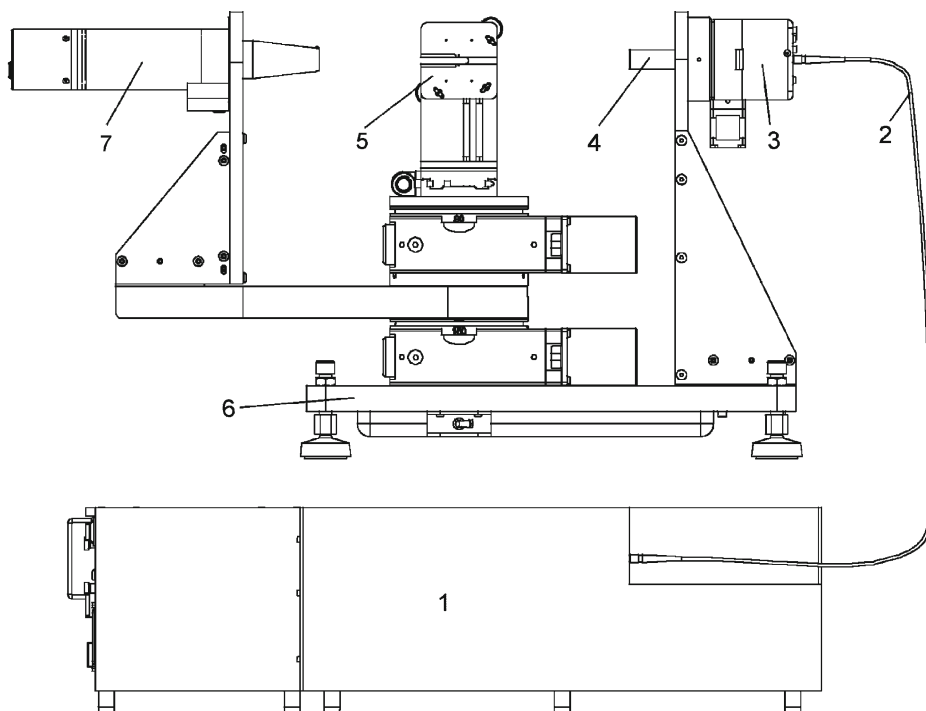


**Figure 2.3.** Schematic (not to scale) of the main components of a variable angle spectroscopic ellipsometer. (1) Monochromator, (2) fiber optic cable, (3) input unit, (4) alignment detector, (5) substrate stage, (6) goniometer base, and (7) detector unit. Note: The control box and the associated computer (for data acquisition and analysis) have been omitted from the diagram. (courtesy of J. A. Woollam Co., Inc.).

and passed through a polarizer (3). Then, the polarized beam interacts with the substrate (mounted on 5) at an oblique angle. Finally, the reflected beam passes through a second polarizer and enters a detector (7). Although many different instrument configurations are available, the data acquisition frequency is generally limited by the rotating element, light source intensity, selected precision of the measurement, wavelengths selected, and angles required for each experiment.

Many ellipsometric adsorption studies have been performed by measuring surfaces *ex situ* in air before and after protein adsorption [56, 70]. These experiments are very simple, allow many substrates (material surface/adsorbed protein) to be measured over a short period of time, and can be performed by minimally trained personnel. However, as pointed out by Arwin [59], this *ex situ* experimental approach involves rinsing and, sometimes, drying steps that introduce the uncertainty of possible desorption and denaturation of proteins before the pertinent measurements.

For this reason, several cells<sup>1</sup> have been designed enabling in situ ellipsometric measurements of protein adsorption processes. In this respect, a widely used design is an open cell assembled of fused silica slides [35] that could be mounted on the vertical substrate-stage of

<sup>1</sup> Unless otherwise noted, the word “cell” in this chapter has been reserved to denominate the chamber in which the adsorption experiment is performed.



the ellipsometer. Arwin's group also designed a cell for total internal reflection ellipsometry under flow injection conditions that can be also used without flow injection as well as with or without stirring [47]. Logothetidis [55] and other research groups [71] have recently reported very interesting results obtained with other cells suited for aqueous liquids (like salty solutions and buffers). Although these designs have proven to be extremely useful, they do not provide information to resolve the question of whether the mass transfer from the bulk or an interfacial process is the determinant step in the protein adsorption rate. To solve this problem, the adsorption experiment can be performed under stagnation conditions. In this case, the axis of the impinging jet intersects perpendicularly to the material surface that is being measured. Stagnation flow cells have been extensively applied to study adsorption kinetics of proteins [72–76], surfactants [77], and polymers [78] using reflectometry, a similar technique.

## 2.5. Material Surface Preparation

Unlike other techniques such as surface plasmon resonance, ellipsometry allows a wide variety of materials to be used as substrates. Gold [79], carbon [80], silicon [49], alumina [81], stainless steel [82], and titania [83] are only a few examples with biomedical relevance. Particularly important are micro/nanophased materials, which promote enhanced interactions with biological molecules. A major problem encountered when performing ellipsometric studies using nanomaterials is, however, that nanophase substrates are typically not suitable for ellipsometry. This is the case for ceramics [4], and material substrates prepared by either dip-coating [84] or electrophoresis [85], which result in rather opaque surfaces, with roughnesses that are several orders of magnitude larger than the nanofeatures themselves. Other techniques such as chemical vapor deposition [86] and direct-current reactive magnetron sputtering [87] offer versatility of fabrication conditions, crystal structure, composition, optical properties, bactericidal abilities, and effective ways to improve the reactivity of the obtained films. However, the cost and complexity of these techniques prevent them from being adopted for general use.

Often, the optical anisotropy observed in polymer thin films [88, 89], self-assembled layers [90], and Langmuir–Blodgett films [91] can be accounted for during the ellipsometric measurement and subsequent modeling. According to our experience, techniques such as sputtering, vaporization (for metallic surfaces), and sol-gel deposition [92–94] have the potential of producing nanometer-thick films with minimum instrument requirements and porosity values that are appropriate for ellipsometry. Other materials such as carbon nanotube (CNT) films can be deposited on a variety of substrates by spin-coating [95], spraying [96], chemical vapor deposition [97], and vacuum filtration [98]. Although they will not be discussed in this chapter, successful examples of ellipsometrically characterized nanostructured films abound in the literature [99–103].

## 2.6. Typical Protein Adsorption Experiment Followed by Ellipsometry

As mentioned in Sects. 2.2 and 2.3 of this chapter, the raw data generated using the ellipsometer are generally expressed in terms of the amplitude ( $\psi$ ) and the phase difference ( $\Delta$ ) as functions of either time ( $t$ ) or wavelength ( $\lambda$ ). These data can be then interpreted using



an optical model, which considers the optical constants ( $n$  and  $k$ ) and thicknesses ( $d$ ) of each layer. Figure 2.4 shows the raw data ( $\psi$  and  $\Delta$  as functions of time) obtained during a typical dynamic adsorption experiment collected at two wavelengths (450 and 650 nm) using spectroscopic ellipsometry.

After fitting the data with an appropriate model, in which the thickness of the protein layer is variable, Figure 2.4 can be expressed in terms of either thickness of the protein layer or surface mass ( $\Gamma$ ), and expanded to include the data collected during a subsequent desorption experiment. Figure 2.5 shows the final plot of the protein adsorption/desorption experiment.

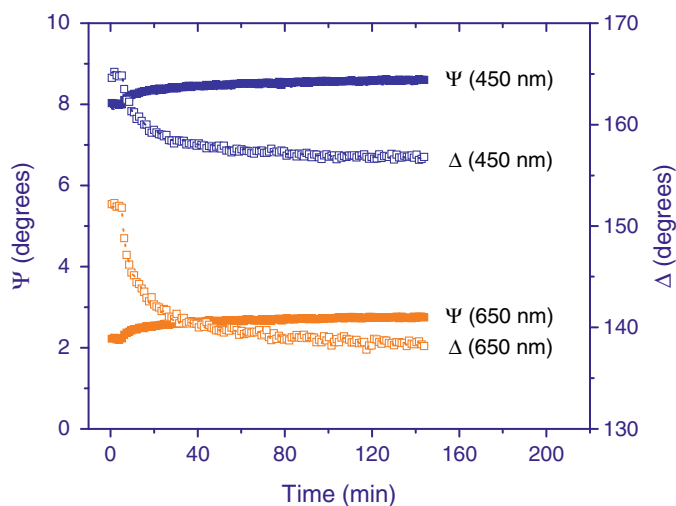


**Figure 2.4.** Typical amplitude ( $\psi$ ) and phase difference ( $\Delta$ ) as functions of time ( $t$ ) collected during an adsorption experiment of 0.1 mg/mL of DAAO to CNT by spectroscopic ellipsometry. Other pertinent conditions are described in Ref. [104].

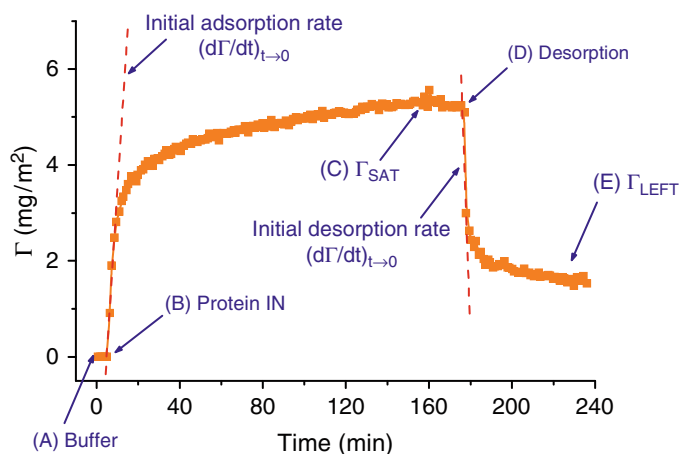


**Figure 2.5.** Typical protein adsorption/desorption experiment monitored by spectroscopic ellipsometry.

Figure 2.5 can be subdivided in five regions. In the first part (A), while only the background electrolyte is pumped through the cell, the initial thickness of the substrate is measured and the baseline stability is verified. In (B), the solution containing protein is introduced and the protein adsorption starts at an initial fast rate process, allowing the calculation of the maximum adsorption rate ( $d\Gamma/dt$ ). As the protein molecules fill the substrate, the adsorption process slows down, reaching a plateau value (C). At this point, the adsorbed amount at saturation ( $\Gamma_{\text{SAT}}$ ), for the designated experimental conditions, can be obtained. In the next region (D), a desorbing agent is introduced into the cell, the adsorbed amount decreases, and the initial desorption rate can be calculated. Finally, in region (E) the amount of protein that remains on the substrate ( $\Gamma_{\text{LEFT}}$ ) can be determined. Additionally, a more accurate value for the optical constants of the substrate and the protein layer before and after desorption can be obtained upon performing spectroscopic scans during stages (A), (C), and (E), respectively.

## 2.7. Ellipsometric Determination of the Adsorption of Proteins to Nanomaterials

So far, this chapter has focused on the importance of studying protein adsorption to nanomaterials surfaces, the most remarkable features of ellipsometry and its instrumental and substrate requirements, as well as the type of data that can be collected in a typical ellipsometric experiment. In the following sections, the most recent results from our laboratory will be discussed. Emphasis will be placed on the adsorption of two proteins (bovine serum albumin [BSA] and D-amino acid oxidase [DAAO]) to two nanostructured materials ( $\text{TiO}_2$  and CNT) deposited on Si/SiO<sub>2</sub> strips.

### 2.7.1. Adsorption of BSA to Nanostructured $\text{TiO}_2$

During the last decades, plain carbon and vanadium–steel orthopedic/dental implants have been gradually replaced by those made of stainless steel, cobalt–chromium alloys, titanium–platinum alloys, and polymeric materials, such as poly(tetrafluoroethylene), poly(methylmethacrylate), polyethylene, and silicones [105]. Because of their biocompatibility and mechanical properties, titanium and titanium-based alloys are one of the most popular materials for medical applications including bone and joint replacements, dental implants, and cardiovascular devices. Since titanium spontaneously generates a surface layer of  $\text{TiO}_2$  when exposed to oxygen-containing environments (such as air or aqueous media), its biocompatibility is dominated by the interaction of cells, tissues, biological fluids, and the oxide layer instead of the metal itself [106].

This phenomenon has been widely recognized and it has motivated recent studies of the interaction of various proteins and  $\text{TiO}_2$  [107, 108]. Among other proteins, BSA has been extensively studied. BSA is a globular protein with an isoelectric point (IEP) of 4.5–5.0, approximate molecular dimensions of  $4 \times 4 \times 14$  nm, and a molecular weight of 66.5 kDa [109]. Because BSA generally undergoes significant structural changes upon adsorption to solid surfaces, it has been considered to be a “soft” protein [10, 11]. Besides its abundance in physiological fluids (such as blood plasma) and physiological functions attributed to albumin (control of osmotic pressure, buffer, and transport), BSA has been also considered a model protein for various biomedically related studies [110–112]. For these reasons, the mechanisms that regulate the adsorption of albumin to nanostructured  $\text{TiO}_2$  surfaces were selected for further analysis in this chapter. In order to attain a better understanding of how

nanostructured surfaces modulate protein–surface interactions, the “real-time” adsorption of BSA to nanostructured  $\text{TiO}_2$  was investigated using spectroscopic ellipsometry [113]. For these experiments, the  $\text{TiO}_2$ -coated substrates were prepared using dip-coating techniques [92–94] and characterized by ellipsometry and atomic force microscopy (AFM). The thickness of the deposited  $\text{TiO}_2$  films was between 1.5 and 3.5 nm. The ellipsometric data were modeled by three uniaxial layers (Si, bulk;  $\text{SiO}_2$   $d = 2.5 \pm 0.5$  nm; and  $\text{TiO}_2$ ) with the optical axis parallel to the silicon wafer substrate. As shown in Figures 2.6 and 2.7, the agreement between the data generated by the optical model, the experimental data, and the topography of the nanostructured  $\text{TiO}_2$  thin films (determined by AFM) was good.

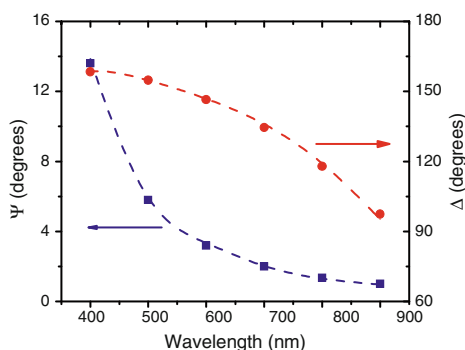


**Figure 2.6.** An example of data ( $\Psi$ , blue; and  $\Delta$ , red) collected from a spectroscopic scan (dots) as well as data generated by the optical model (lines). Other pertinent conditions for this experiment are described in Ref. [113].

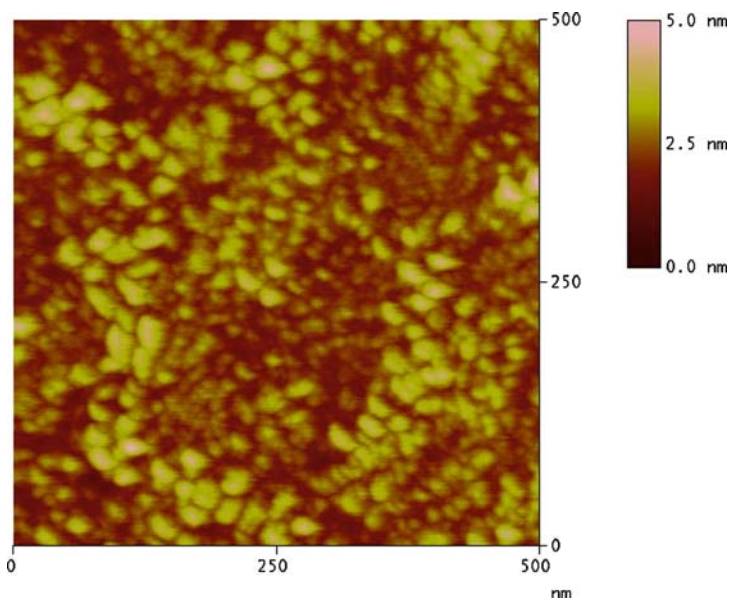


**Figure 2.7.** AFM image of a representative thin-film of  $\text{TiO}_2$  deposited on a silica wafer. Other pertinent conditions for this experiment are described in Ref. [113].

As shown in Figures 2.8 and 2.9, both the adsorbed amount and the adsorption rate of BSA to nanostructured  $\text{TiO}_2$  increased as a function of the protein concentration in the 0.001–0.1 mg/mL range.

Although the interaction of BSA on  $\text{TiO}_2$  was not affected by the ionic strength of the protein solution, greater amounts of BSA were adsorbed at the IEP. This behavior can be explained by considering that, at the IEP, the adsorbed molecules minimize electrostatic repulsions, attain closer packing [114], and retain their native structure. The results collected by ellipsometry indicate that BSA adsorbed to nanostructured  $\text{TiO}_2$  formed a monolayer with a (more or less) compact arrangement. In agreement with a rather general phenomenon in protein adsorption [115], formation of the BSA adsorbed layer was driven by a combination

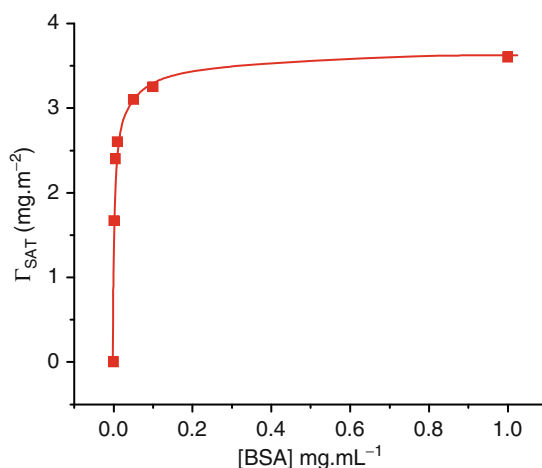


**Figure 2.8.** Effect of the protein concentration on the amount of BSA adsorbed on nanostructured  $\text{TiO}_2$ . Other pertinent conditions of this experiment are described in Ref. [113].

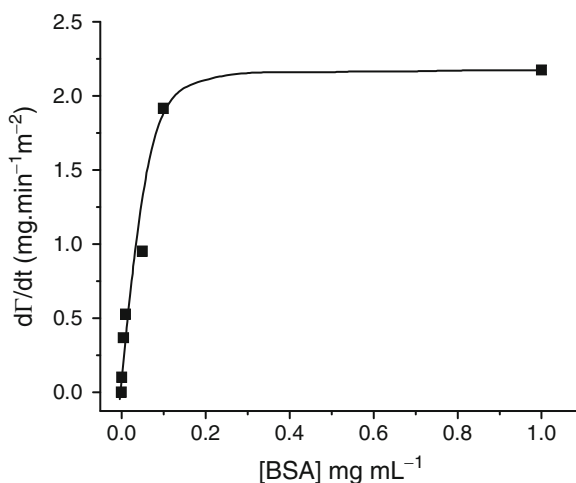


**Figure 2.9.** Effect of the protein concentration on the initial adsorption rate of BSA on nanostructured  $\text{TiO}_2$ . Other pertinent conditions of this experiment are described in Ref. [113].

of hydrophobic (mainly) and hydrophilic interactions. Data collected by ellipsometry indicated that protein layers in the 2–5-nm thickness range were obtained; this result suggests that, upon adsorption to nanostructured films of  $\text{TiO}_2$ , BSA undergoes (at least some) structural changes.

The aforementioned results highlight the utility of spectroscopic ellipsometry to investigate not only the optical properties of nanostructured materials, but also the adsorption of proteins to such layers. More information regarding adsorption of BSA to nanostructured  $\text{TiO}_2$  can be found in Ref. [113].

### 2.7.2. Adsorption of Proteins to Carbon Nanotubes: Biosensing Applications

Sensitive, selective, and cost-effective analysis of biomolecules is important in clinical diagnostics and treatment. Among others, electrochemical biosensors based on enzyme-modified electrodes are very attractive because they integrate the selectivity of enzymatic reactions with highly sensitive electrochemical signal transduction [116–118]. Biosensors are currently applied in the clinical [116, 118], environmental [119, 120], agricultural [117], and pharmaceutical fields. Although different nanomaterials can be used as substrates [121], carbon nanotubes (CNT) have an enormous potential because they can act simultaneously as immobilization matrices and as electrochemical transducers [122–128]. In addition, CNT are stable over a large range of potentials, are catalytically active toward many electrochemical reactions [127–130], and provide a significant increase in electrode area [129]. Although considerable progress has been made by encapsulating or cross-linking enzymes [131–133], the analytical performance of CNT biosensors still suffers from some fundamental deficiencies such as slow response ( $\geq 10$  s) and limited sensitivity (approximately micromolar).

In order to better understand the driving forces and consequences of the interaction of proteins with CNT, preliminary studies were performed by reflectometry using BSA as a model protein [74]. According to those results, BSA molecules arriving to the CNT surface adopted a preferred orientation with the positive and nonpolar patches of the protein facing the hydrophobic sorbent surface; this arrangement resulted in an attachment-controlled adsorption process. Even under electrostatically unfavorable conditions, dehydration of both the CNT surface and the nonpolar regions of BSA promoted adsorption on CNT. At steady state conditions, a layer of BSA adsorbed to CNT (at the IEP of the protein) resembled a close-packed monolayer of protein molecules. At pH values away from the IEP, repulsive protein–protein interactions prevailed over attractive surface–protein interactions, limiting the amount of BSA adsorbed to the CNT layer.

More recently, our group described the interaction of CNT with D-amino acid oxidase (EC 1.4.3.3, DAAO) [104]. DAAO is a dimeric protein of approximately 80.6 kDa that exhibits an elongated ellipsoidal framework with approximate dimensions of 11 nm (length)  $\times$  4 nm (width) [134] and an IEP in the 6.3 [135] to 7.0 [136] range. DAAO is of particular interest because it recognizes functional groups, instead of a specific analyte [137, 138]. Therefore, combining DAAO with a separation technique such as capillary electrophoresis should increase the versatility of the sensor, allowing detection of several analytes with similar structure. Although the biological role of DAAO in animals is not clear yet, recent progress in the detection of D-amino acids has linked DAAO to aging [139, 140] and pathological conditions such as schizophrenia [141, 142], epilepsy, Alzheimer's disease, and renal diseases [143]. Additionally, understanding the adsorption mechanisms of DAAO to solid surfaces would enable developing more efficient catalysts for biomedical applications [144–146]. Consequently, understanding the driving forces for the adsorption of DAAO to

CNT would enable the rational design of biosensors and biocatalysts, avoiding harsh immobilization conditions and trapping membranes [147, 148].

Dynamic adsorption/desorption experiments of DAAO to CNT were performed as a function of the protein concentration, pH, and ionic strength. In general, all adsorption experiments exhibited a similar general behavior: (1) adsorption of DAAO to the CNT surface was a single step process; (2) adsorbed DAAO was not significantly affected by rinsing the substrate with buffer; and (3) part of the adsorbed DAAO was removed by rinsing with 4 mM sodium dodecyl sulfate (SDS). An example of the data collected during such adsorption/desorption experiments is shown in Figure 2.5. Neither the desorption kinetics nor the amount of protein remaining attached to the CNT surface was affected by the amount of DAAO adsorbed ( $\Gamma_{\text{SAT}}$ ). Based on these experimental observations, the overall adsorption process could be interpreted as the sum of two different populations of DAAO on the CNT surface: one that is removable by SDS ( $\Gamma_1$ ), and another ( $\Gamma_2$ ) that remains attached to the surface even after washing with surfactant.

Thickness values of the adsorbed DAAO obtained with spectroscopic ellipsometry analysis indicate that DAAO can adopt multiple orientations, either horizontal or tilted at different angles with respect to the CNT surface (Figure 2.10). It was also observed that higher amounts of DAAO were adsorbed at the IEP of the DAAO; moreover, the initial adsorption rate and the population of DAAO loosely attached ( $\Gamma_1$ ) to the CNT surface increase as the bulk protein concentration increases. More importantly, measurements of the enzymatic activity of the adsorbed protein (Figure 2.10) provided evidence that the enzymatic activity correlated with the adsorbed amount of protein when the adsorption reaction was performed under attractive electrostatic conditions. However, CNT surfaces modified with DAAO at, or above, the IEP of the protein displayed lower enzymatic activity.

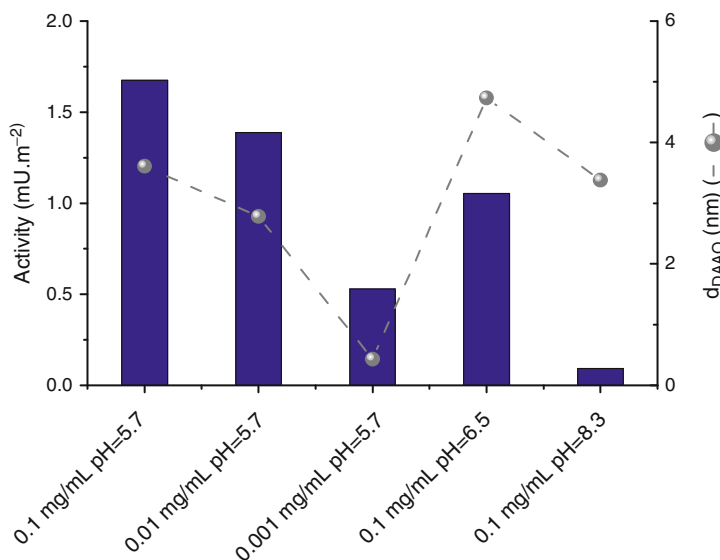


**Figure 2.10.** Comparison between the enzymatic activity and amount of DAAO adsorbed to CNT under different experimental conditions. The *dashed line* was included with the sole purpose of connecting the DAAO thickness values ( $d_{\text{DAAO}}$ ). Other pertinent conditions for this experiment are described in Ref. [104].

If one considers that proteins generally display higher structural stability (and, therefore, a smaller tendency to spread at the IEP) [114], these results may suggest that, despite the amount adsorbed, DAAO could undergo small changes in orientation rather than changes in structural conformation on the CNT surface. These changes in orientation are responsible for the observed differences in the biological activity of the adsorbed protein; for this reason, not only the surface and the protein [149], but also the adsorption conditions dictate the biological activity of a protein adsorbed on a CNT surface. More information regarding adsorption of DAAO to CNT surfaces can be found in Ref. [104].

## 2.8. Innovative Applications

Recent developments in instrumentation and data analysis software have enabled ellipsometry to transcend the boundaries of traditional physics, engineering, and chemistry settings. In this respect, several biomedical applications have been recently reported. For example, Schulz et al. [150] demonstrated that spectroscopic ellipsometry is a suitable optical tool to investigate biological specimens such as liver tissue, human nails, and human skin. These researchers performed a hydration study that revealed changes of the optical constants upon hydration and dehydration of nails and liver. The very different dehydration time scales for nails and liver provided evidence of the importance of the keratin matrix as a water barrier [150]. Danny et al. later extended this study to investigate the optical properties of various layers of human skin. In this case, the evolution of  $\psi$  and  $\Delta$  were described using a morphological model containing an effective medium approximation accounting for the water content of the skin, surface roughness of corneocytes, and the alternating lipid layers in the skin [151].

Cardenas et al. recently applied ellipsometry to investigate the amount, thickness, and structure of films formed by human whole saliva on alumina surfaces [81]. Their analyses were complemented by means of neutron reflectivity and AFM, and showed that saliva adsorbed rapidly on alumina. Such a film could be modeled by two layers: (1) an inner, dense, and thin region that formed a uniform layer and (2) a second layer, more diffuse and thicker, which protruded toward the bulk of the solution. The thickness of both layers of a salivary film formed on sapphire was found to be on the order of a few hundreds of Ångströms [81]. Researchers from the same laboratory also investigated the adsorption of two salivary mucins (specifically, structure and topography) under conditions similar to those found in the oral cavity in terms of ionic strength, pH, and protein concentration [152]. In this case, the salivary protein film was described as a two-sublayer structure in which an inner, dense layer was decorated by large aggregates of proteins. The shape and height of these large aggregates largely depended on the type of substrata tested. Additionally, Santos et al. showed that adsorption of a human salivary mucin (MUC5B) was controlled by the type of substrata; in this case, film topography was similar to that of the larger aggregates present in the salivary films. According to these results, MUC5B molecules adsorbed on hydrophobic substrates were especially resistant to both elution with buffer solution and SDS. Therefore, these large mucins can be responsible for the increased resistance of the saliva films on hydrophobic substrates. Mucins could then protect the intraoral surfaces against surface-active components present in oral health care products. These results are also in line with the adsorption of other salivary proteins to biological materials [152].

Ellipsometry has also been applied in the development of various biosensors. Several of these sensors were reviewed by Arwin [153]. Attractive features for ellipsometric sensors



are the high resolution of the thickness of the adsorbed protein layer and the possibility of performing in situ measurements using nonlabeled molecules. According to the type of sensing mechanism used, ellipsometric sensors were classified in terms of affinity layer (analyte interacts with a sensing layer deposited on a substrate, resulting in a change in thickness of the protein layer), matrix layer (analyte diffuses inside a thin layer deposited on a substrate, resulting in a change in the refractive index), integrating layer (analyte interacts with a surface resulting in an accumulated thickness change over time), and a homogeneous layer (optical properties of the layer change upon interaction with the analyte) [153]. Among other ellipsometric sensors, Demirel et al. [154] investigated the effects of several variables on the formation of self-assembled monolayers of 3-mercaptopropyltrimethoxysilane on Si surfaces. Such surfaces were then modified with oligodeoxynucleotides and used to detect hybridization by ellipsometry. Other studies involving DNA adsorption and subsequent interactions have been also reported [155–157]. Using a micropatterned panel of seven lectins, Carlsson et al. [158] discriminated different meat juices from cattle, chicken, pig, cod, turkey, and lamb. In this case, biorecognition was evaluated with null ellipsometry and the data obtained were related to lactoferrin, an internal standard. Furthermore, the patterns of lectins binding to the meat proteins were visualized by scanning ellipsometry [158].

One of the most exciting areas in ellipsometry research is the development of imaging ellipsometry, which enabled quantification and visualization of the lateral thickness distribution of thin protein layers formed on solid substrates [38]. Biosensors based on imaging ellipsometry combine the specificity of biomolecular interactions with protein-patterned surfaces and have the advantages of high spatial resolution, fast data acquisition, and simplicity of use [159]. In this respect, van Noort et al. [160] reported the fabrication of an affinity biochip with a matrix of 900 targets for detection of binding events of carbohydrates with lectins using imaging ellipsometry. More recently, an immunosensor based on imaging ellipsometry was developed for the detection of *Legionella pneumophila* [161]. The sensor was fabricated by sequential deposition of 11-mercaptoundecanoic acid, protein G, and a monoclonal antibody. Imaging ellipsometry was then used to detect binding of *L. pneumophila* to the antibody layer; the limit of detection in this case was approximately  $10^3$  colony-forming units/ml [161]. Similar results were obtained when *Salmonella typhimurium* [162] and *Yersinia enterocolitica* [163] were examined. Comparable approaches have been also used to detect *Arthrobacter oxydans* [164] and dengue virus particles [165], to investigate the orientation of human immunoglobulin G [166], and to visualize two neutralizing human monoclonal antibodies from patients infected with severe acute respiratory syndrome coronavirus [167].

Yu and Jin [79] recently combined ellipsometry with electrochemical methods for studying electrostatic interactions of proteins and solid surfaces. These researchers provided evidence that the rate of fibrinogen adsorption on a potentiostatic surface was faster than that observed on the non-potentiostatic surface and concluded that hydrophobic interactions were the major driving force for the observed adsorption of fibrinogen to gold. Descriptions of other biomedical applications of imaging ellipsometry abound in the literature [168–171].

## 2.9. Conclusions

In this chapter, the basic concepts behind ellipsometry and spectroscopic ellipsometry were discussed along with some pertinent instrument details. Particular emphasis was placed on experimental details related to the development of medically relevant bioconjugated

surfaces. In this regard, ellipsometry has enabled collecting real-time data related to a wide variety of biological processes. When complemented with other techniques such as electron and fluorescence microscopy, circular dichroism, infrared spectroscopy, AFM, and quartz crystal microbalance, ellipsometry enables a rational interpretation of the microstructure of layers of protein adsorbed on material surfaces. Original papers investigating live tissues as well as imaging ellipsometry should open new possibilities for applications in the biomedical field. Clearly, opportunities abound for fundamental discovery as well as for breakthroughs in applications that involve proteins and biomaterials, biotechnology, and nanotechnology.

## Acknowledgments

The authors would like to thank the Southwest Research Institute for providing access to their atomic force microscope. Financial support for this project was provided in part by The University of Texas at San Antonio, the National Institute of General Medical Sciences (NIGMS)/National Institutes of Health (1SC3GM081085), and the Morrison Trust.

## References

1. Nakanishi K, Sakiyama T, Imamura K. On the adsorption of proteins on solid surfaces, a common but very complicated phenomenon. *J. Biosci. Bioeng.* 2001;91:233–244.
2. Lynch I, Dawson KA. Protein-nanoparticle interactions. *Nano Today* 2008;3:40–47.
3. Cheng M-D. Effects of nanophase materials (<20 nm) on biological responses. *J. Environ. Sci. Health* 2005;39:2691–2705.
4. Webster TJ, Ergun C, Doremus RH, Siegel RW, Bizios R. Specific proteins mediate enhanced osteoblast adhesion on nanophase ceramics. *J. Biomed. Mater. Res.* 2000;51:475–483.
5. Cheng F-Y, Wang SP-H, Su C-H, Tsai T-L, Wu P-C, Shieh D-B, et al. Stabilizer-free poly(lactide-co-glycolide) nanoparticles for multimodal biomedical probes. *Biomaterials* 2008;29:2104–2112.
6. Chung Y-C, Chen IH, Chen C-J. The surface modification of silver nanoparticles by phosphoryl disulfides for improved biocompatibility and intracellular uptake. *Biomaterials* 2008;29:1807–1816.
7. Deng C, Chen J, Chen X, Xiao C, Nie L, Yao S. Direct electrochemistry of glucose oxidase and biosensing for glucose based on boron-doped carbon nanotubes modified electrode. *Biosens. Bioelectron.* 2008;23:1272–1277.
8. Engel E, Michiardi A, Navarro M, Lacroix D, Planell JA. Nanotechnology in regenerative medicine: the materials side. *Trends Biotechnol.* 2008;26:39–47.
9. Liu H, Webster TJ. Nanomedicine for implants: a review of studies and necessary experimental tools. *Biomaterials* 2007;28:354–369.
10. Norde W. Driving forces for protein adsorption at solid surfaces. In: Malmsten M, (ed.) *Biopolymers at Interfaces*. New York: Marcel Dekker; 2003.
11. Norde W. My voyage of discovery to proteins in flatland and beyond. *Colloids Surf. B Biointerfaces* 2008;61:1–9.
12. Larsericsdotter H, Oscarsson S, Buijs J. Thermodynamic analysis of lysozyme adsorbed to silica. *J. Colloid Interface Sci.* 2004;276:261–268.
13. Giacomelli CE, Norde W. The adsorption-desorption cycle. Reversibility of the BSA-Silica system. *J. Colloid Interface Sci.* 2001;233:234–240.
14. Norde W, Zoungrana T. Surface-induced changes in the structure and activity of enzyme physically immobilized at solid/liquid interfaces. *Biotechnol. Appl. Biochem.* 1998;28:133–143.
15. Giacomelli CE, Norde W. Structural changes in proteins resulting from homomolecular exchange at solid surfaces. In: Hubbard AT, (ed.) *Encyclopedia of Surface and Colloid Science*. New York: Marcel Dekker; 2003.
16. van der Veen M, Stuart MC, Norde W. Spreading of proteins and its effect on adsorption and desorption kinetics. *Colloids Surf. B Biointerfaces* 2007;54:136–142.
17. Bernabeu P, Tamisier L, De Cesare A, Caprani A. Study of the adsorption of albumin on a platinum rotating disk electrode using impedance measurements. *Electrochim. Acta* 1988;33:1129–1136.

18. Zhang Y, Fung Y, Sun H, Zhu D, Yao S. Study of protein adsorption on polymer coatings surface by combining quartz crystal microbalance with electrochemical impedance methods. *Sens. Actuators B Chem* 2005;108:933–942.
19. Gray JJ. The interaction of proteins with solid surfaces. *Curr. Opin. Struct. Biol.* 2004;14:110–115.
20. Sapsford KE, Ligler FS. Real-time analysis of protein adsorption to a variety of thin films. *Biosens. Bioelectron.* 2004;19:1045–1055.
21. Baszkim A, Norde W, (eds.). *Physical Chemistry of Biological Interfaces*. New York, NY: Marcel Dekker; 2000.
22. Griesser HJ, Kingshott P, McArthur SL, McLean KM, Kinsel GR, Timmons RBRB. Surface-MALDI mass spectrometry in biomaterials research. *Biomaterials* 2004;25:4861–4875.
23. Yang K, Sun Y. Optics-intrinsic double-circle phenomenon in protein adsorption visualized by confocal laser scanning microscopy. *Biochem. Eng. J.* 2008;39:258–266.
24. Lu JR, Zhao X, Yaseen M. Protein adsorption studied by neutron reflection. *Curr. Opin. Colloid Interface Sci.* 2007;12:9–16.
25. Reich Z, Kapon R, Nevo R, Pilpel Y, Zmora S, Scolnik Y. Scanning force microscopy in the applied biological sciences. *Biotechnol. Adv.* 2001;19:451–485.
26. Teichroeb JH, Forrest JA, Jones LW, Chan J, Dalton K. Quartz crystal microbalance study of protein adsorption kinetics on poly(2-hydroxyethyl methacrylate). *J. Colloid Interface Sci.* 2008;325:157–164.
27. Dolatshahi-Pirouz A, Rechendorff K, Hovgaard MB, Foss M, Chevallier J, Besenbacher F. Bovine serum albumin adsorption on nano-rough platinum surfaces studied by QCM-D. *Colloids Surf. B Biointerfaces* 2008;66:53–59.
28. Wertz CF, Santore MM. Adsorption and relaxation kinetics of albumin and fibrinogen on hydrophobic surfaces: single-species and competitive behavior. *Langmuir* 1999;15:8884–8894.
29. Wertz CF, Santore MM. Effect of surface hydrophobicity on adsorption and relaxation kinetics of albumin and fibrinogen: single-species and competitive behavior. *Langmuir* 2001;17:3006–3016.
30. Righetti PG, Gelfi C, Verzola B, Castelletti L. The state of the art of dynamic coatings. *Electrophoresis* 2001;22:603–611.
31. Verzola B, Gelfi C, Righetti PG. Quantitative studies on the adsorption of proteins to the bare silica wall in capillary electrophoresis: II. Effects of adsorbed, neutral polymers on quenching the interaction. *J. Chromatogr. A* 2000;874:293.
32. Castelletti L, Verzola B, Gelfi C, Stoyanov A, Righetti PG. Quantitative studies on the adsorption of proteins to the bare silica wall in capillary electrophoresis: III: effects of adsorbed surfactants on quenching the interaction. *J. Chromatogr. A* 2000;894:281–289.
33. Olivier JC, Taverna M, Vauthier C, Couvreur P, Baylocq-Ferrier D. Capillary electrophoresis monitoring of the competitive adsorption of albumin onto the orosomucoid-coated polyisobutylcyanoacrylate nanoparticles. *Electrophoresis* 1994;15:234–239.
34. Fujiwara H. *Spectroscopic Ellipsometry. Principles and Applications*. West Sussex, England: Wiley; 2007.
35. Arwin H. Spectroscopic ellipsometry and biology: recent developments and challenges. *Thin Solid Films* 1998;313–314:764–774.
36. Höök F, Vörös J, Rodahl M, Kurrat R, Böni P, Ramsden JJ, et al. A comparative study of protein adsorption on titanium oxide surfaces using in situ ellipsometry, optical waveguide lightmode spectroscopy, and quartz crystal microbalance/dissipation. *Colloids Surf. B* 2002;24:155–170.
37. Pak HK, Law BM. 2D imaging ellipsometric microscope. *Rev. Sci. Instrum.* 1995;66:4972–4976.
38. Jin G, Jansson R, Arwin H. Imaging ellipsometry revisited: developments for visualization of thin transparent layers on silicon substrates. *Rev. Sci. Instrum.* 1996;67:2930.
39. Linke F, Merkel R. Ellipsometric microscopy: developments towards biophysics. *IEE Proc Nanobiotechnol* 2004;151:95.
40. Linke F, Merkel R. Quantitative ellipsometric microscopy at the silicon–air interface. *Rev. Sci. Instrum.* 2005;76:063701.
41. Tompkins HG. *A User's Guide to Ellipsometry*. San Diego, CA: Academic Press; 1993.
42. Greef R. Ellipsometry in electrochemistry: a spectrum of applications. *Thin Solid Films* 1993;233:32–39.
43. Aspnes DE. Expanding horizons: new developments in ellipsometry and polarimetry. *Thin Solid Films* 2004;455–456:3–13.
44. Tompkins HG, Irene EA, (eds.). *Handbook of Ellipsometry*. Norwich, NY: W' Andrew; 2005.
45. Spaeth K, Brecht A, Gauglitz G. Studies on the biotin-avidin multilayer adsorption by spectroscopic ellipsometry. *J. Colloid Interface Sci.* 1997;196:128–135.
46. Karlsson LM, Schubert M, Ashkenov N, Arwin H. Protein adsorption in porous silicon gradients monitored by spatially-resolved spectroscopic ellipsometry. *Thin Solid Films* 2004;455–456:726–730.

47. Poksinski M, Arwin H. Protein monolayers monitored by internal reflection ellipsometry. *Thin Solid Films* 2004;455–456:716–721.
48. Feller L, Bearinger JP, Wu L, Hubbell JA, Textor M, Tosatti S. Micropatterning of gold substrates based on poly(propylene sulfide-bl-ethylene glycol), (PPS-PEG) background passivation and the molecular-assembly patterning by lift-off (MAPL) technique. *Surf. Sci.* 2008;602:2305–2310.
49. Goyal DK, Pribil GK, Woollam JA, Subramanian A. Detection of ultrathin biological films using vacuum ultraviolet spectroscopic ellipsometry. *Mater. Sci. Eng. B* 2008;149:26–33.
50. Nabok AV, Tsargorodskaya A, Holloway A, Starodub NF, Gojster O. Registration of T-2 mycotoxin with total internal reflection ellipsometry and QCM impedance methods. *Biosens. Bioelectron.* 2007;22:885–890.
51. Aroulmoji V, Aguié-Béghin V, Mathlouthi M, Douillard R. Effect of sucrose on the properties of caffeine adsorption layers at the air/solution interface. *J. Colloid Interface Sci.* 2004;276:269–276.
52. Nabok AV, Tsargorodskaya A, Hassan AK, Starodub NF. Total internal reflection ellipsometry and SPR detection of low molecular weight environmental toxins. *Appl. Surf. Sci.* 2005;246:381–386.
53. Logothetidis S, Gioti M, Lousinian S, Fotiadou S. Haemocompatibility studies on carbon-based thin films by ellipsometry. *Thin Solid Films* 2005;482:126–132.
54. Liu Y, Li Z, He Z, Chen D, Pan S. Structure and blood compatibility of tetrahedral amorphous hydrogenated carbon formed by a magnetic-field-filter plasma stream. *Surf. Coat. Technol.* 2007;201:6851–6856.
55. Lousinian S, Logothetidis S. Optical properties of proteins and protein adsorption study. *Microelectron. Eng.* 2007;84:479–485.
56. Lousinian S, Logothetidis S, Laskarakis A, Gioti M. Haemocompatibility of amorphous hydrogenated carbon thin films, optical properties and adsorption mechanisms of blood plasma proteins. *Biomol. Eng.* 2007;24:107–112.
57. Lousinian S, Kassavetis S, Logothetidis S. Surface and temperature effect on fibrinogen adsorption to amorphous hydrogenated carbon thin films. *Diamond Relat. Mater.* 2007;16:1868–1874.
58. Keuren JFW, Wielders SJH, Willems GM, Morra M, Cahalan L, Cahalan P, et al. Thrombogenicity of polysaccharide-coated surfaces. *Biomaterials* 2003;24:1917–1924.
59. Arwin H. Ellipsometry on thin organic layers of biological interest: characterization and applications. *Thin Solid Films* 2000;377–378:48–56.
60. Russev SC, Arguirov TV, Gurkov TD.  $\beta$ -Casein adsorption kinetics on air-water and oil-water interfaces studied by ellipsometry. *Colloids Surf. B* 2000;19:89–100.
61. Bae YM, Oh B-K, Lee W, Lee WH, Choi J-W. Study on orientation of immunoglobulin G on protein G layer. *Biosens. Bioelectron.* 2005;21:103–110.
62. Vinnichenko M, Gago R, Huang N, Leng YX, Sun H, Kreissig U, et al. Spectroscopic ellipsometry investigation of amorphous carbon films with different sp<sup>3</sup> content: relation with protein adsorption. *Thin Solid Films* 2004;455–456:530–534.
63. Karlsson LM, Tengvall P, Lundström I, Arwin H. Penetration and loading of human serum albumin in porous silicon layers with different pore sizes and thicknesses. *J. Colloid Interface Sci.* 2003;266:40–47.
64. Tsargorodskaya A, Nabok AV, Ray AK. Ellipsometric study of the adsorption of bovine serum albumin into porous silicon. *Nanotechnology* 2004;15:703–709.
65. De Feijter JA, Benjamins J, Veer FA. Ellipsometry as a tool to study the adsorption behavior of synthetic and biopolymers at the air-water interface. *Biopolymers* 1978;17:1759–1772.
66. Lassen B, Malmsten M. Competitive protein adsorption studied with TIRF and ellipsometry. *J. Colloid Interface Sci.* 1996;179:470–477.
67. Kurrat R, Prenosil JE, Ramsden JJ. Kinetics of human and bovine serum albumin adsorption at silica-titania surfaces. *J. Colloid Interface Sci.* 1997;185:1–8.
68. Giacomelli CE, Esplandiú MJ, Ortiz PI, Avena MJ, De Pauli CP. Ellipsometric study of bovine serum albumin adsorbed onto Ti/TiO<sub>2</sub> electrodes. *J. Colloid Interface Sci.* 1999;218:404–411.
69. Vinnichenko M, Gago R, Huang N, Leng YX, Sun H, Kreissig U, et al. Spectroscopic ellipsometry investigation of amorphous carbon films with different sp<sup>3</sup> content: relation with protein adsorption. *Thin Solid Films* 2004;455–456:530–534.
70. Foose LL, Blanch HW, Radke CJ. Immobilized protein films for assessing surface proteolysis kinetics. *J. Biotechnol.* 2007;132:32–37.
71. Brétagnot F, Kylián O, Hasiwa M, Ceriotti L, Rauscher H, Ceccone G, et al. Micro-patterned surfaces based on plasma modification of PEO-like coating for biological applications. *Sens. Actuators B* 2007;123:283–292.
72. Riquelme BD, Valverde JR, Rasia RJ. Kinetic study of antibody adhesion on a silicon wafer by laser reflectometry. *Optic. Laser Eng.* 2003;39:589–598.
73. Elgersma AV, Zsom RLJ, Lyklema J, Norde W. Kinetics of single and competitive protein adsorption studied by reflectometry and streaming potential measurements. *Colloids Surf. A* 1992;65:17–28.

74. Valenti LE, Fiorito PA, Garcia CD, Giacomelli CE. The adsorption-desorption process of bovine serum albumin on carbon nanotubes. *J. Colloid Interface Sci.* 2007;307:349–356.
75. de Vos WM, Biesheuvel PM, de Keizer A, Kleijn JM, Cohen Stuart MA. Adsorption of the protein bovine serum albumin in a planar poly(acrylic acid) brush layer as measured by optical reflectometry. *Langmuir* 2008;24:6575–6584.
76. Hofs B, Brzozowska A, de Keizer A, Norde W, Cohen Stuart MA. Reduction of protein adsorption to a solid surface by a coating composed of polymeric micelles with a glass-like core. *J. Colloid Interface Sci.* 2008;325:309–315.
77. Atkin R, Craig VS, Wanless EJ, Biggs S. The influence of chain length and electrolyte on the adsorption kinetics of cationic surfactants at the silica-aqueous solution interface. *J. Colloid Interface Sci.* 2003;266:236–244.
78. Dijt JC, Stuart MAC, Fleer GJ. Reflectometry as a tool for adsorption studies. *Adv. Colloid Interface Sci.* 1994;50:79–101.
79. Yu Y, Jin G. Influence of electrostatic interaction on fibrinogen adsorption on gold studied by imaging ellipsometry combined with electrochemical methods. *J. Colloid Interface Sci.* 2005;283:477–481.
80. Logothetidis S. Haemocompatibility of carbon based thin films. *Diamond Relat. Mater.* 2007;16:1847–1857.
81. Cardenas M, Arnebrant T, Rennie A, Fragneto G, Thomas RK, Lindh L. Human saliva forms a complex film structure on alumina surfaces. *Biomacromolecules* 2007;8:65–69.
82. Vinnichenko M, Chevolleau T, Pham MT, Poperenko L, Maitz MF. Spectroellipsometric, AFM and XPS probing of stainless steel surfaces subjected to biological influences. *Appl. Surf. Sci.* 2002;201:41–50.
83. Advincula M, Fan X, Lemons J, Advincula R. Surface modification of surface sol-gel derived titanium oxide films by self-assembled monolayers (SAMs) and non-specific protein adsorption studies. *Colloids Surf. B* 2005;42:29–43.
84. Jihua Y, David SW, Keith CG, McQuillan AJ. Electronic states and photoexcitation processes of titanium dioxide nanoparticle films dip coated from aqueous Degussa P25 photocatalyst suspension. *J. Appl. Phys.* 2007;101:023714.
85. Besra L, Liu M. A review on fundamentals and applications of electrophoretic deposition (EPD). *Prog. Mater. Sci.* 2007;52:1–61.
86. Vahlas C, Caussat B, Serp P, Angelopoulos GN. Principles and applications of CVD powder technology. *Mater. Sci. Eng. R* 2006;53:1–72.
87. Tanemura S, Miao L, Wunderlich W, Tanemura M, Mori Y, Toh S, et al. Fabrication and characterization of anatase/rutile-TiO<sub>2</sub> thin films by magnetron sputtering: a review. *Sci. Technol. Adv. Mater.* 2005;6:11–17.
88. Losurdo M, Bruno G, Irene EA. Anisotropy of optical properties of conjugated polymer thin films by spectroscopic ellipsometry. *J. Appl. Phys.* 2003;94:4923–4929.
89. Winfield JM, Donley CL, Ji-Seon K. Anisotropic optical constants of electroluminescent conjugated polymer thin films determined by variable-angle spectroscopic ellipsometry. *J. Appl. Phys.* 2007;102:063505.
90. Styrkas DA, Keddle JL, Lu JR, Su TJ, Zhdan PA. Structure of self-assembled layers on silicon: combined use of spectroscopic variable angle ellipsometry, neutron reflection, and atomic force microscopy. *J. Appl. Phys.* 1999;85:868.
91. Lecourt B, Blaudez D, Turlet JM. Anisotropy in Langmuir–Blodgett films studied by generalized spectroscopic ellipsometry. *Thin Solid Films* 1998;313–314:790–794.
92. Fan Q, McQuillin B, Ray AK, Turner ML, Seddon AB. High density, non-porous anatase titania thin films for device applications. *J. Phys. D Appl. Phys.* 2000;33:2683–2686.
93. Biju KP, Jain MK. Sol-gel derived TiO<sub>2</sub>:ZrO<sub>2</sub> multilayer thin films for humidity sensing application. *Sens. Actuators B* 2008;128:407–413.
94. Radha G, Ashok K. Bioactive materials for biomedical applications using sol-gel technology. *Biomed. Mater.* 2008;034005.
95. Jung HY, Jung SM, Suh JS. Horizontally aligned single-walled carbon nanotube field emitters fabricated on vertically aligned multi-walled carbon nanotube electrode arrays. *Carbon* 2008;46:1345–1349.
96. Barnes TM, van de Lagemaat J, Levi D, Rumbles G, Coutts TJ, Weeks CL, et al. Optical characterization of highly conductive single-wall carbon-nanotube transparent electrodes. *Phys. Rev. B* 2007;75:23541001–2354110.
97. Elim HI, Ji W, Ma GH, Lim KY, Sow CH, Huan CHA. Ultrafast absorptive and refractive nonlinearities in multi-walled carbon nanotube film. *Appl. Phys. Lett.* 2004;85:1799–1801.
98. Fanchini G, Miller S, Parekh BB, Chhowalla M. Optical anisotropy in single-walled carbon nanotube thin films: implications for transparent and conducting electrodes in organic photovoltaics. *Nano Lett.* 2008;8:2176–2179.

99. Wakita K, Abe K, Shim Y, Mamedov N. Spectroscopic ellipsometry of powdered CuInS<sub>2</sub> with nanowires. *Thin Solid Films* 2006;499:285–288.
100. Gilliot M, En Naciri A, Johann L, d'Orleans C, Muller D, Stoquert JP, et al. Application of spectroscopic ellipsometry to the investigation of the optical properties of cobalt-nanostructured silica thin layers. *Appl. Surf. Sci.* 2006;253:389–394.
101. Bhat RR, Genzer J. Using spectroscopic ellipsometry for quick prediction of number density of nanoparticles bound to non-transparent solid surfaces. *Surf. Sci.* 2005;596:187–196.
102. Losurdo M. Relationships among surface processing at the nanometer scale, nanostructure and optical properties of thin oxide films. *Thin Solid Films* 2004;455–456:301–312.
103. Takeda Y, Plaksin OA, Wang H, Kishimoto N. Optical nonlinearity of Au nanoparticles fabricated by negative ion implantation. *Nucl. Instrum. Methods Phys. Res. B* 2007;257:47–50.
104. Mora MF, Giacomelli CE, Garcia CD. Interaction of D-amino acid oxidase to carbon nanotubes: implications in the design of biosensors. *Anal. Chem.* 2009;81:1016–1022.
105. Williams DF. On the mechanisms of biocompatibility. *Biomaterials* 2008;29:2941–2953.
106. Giacomelli CE, Avena MJ, De Pauli CP. Adsorption of bovine serum albumin onto TiO<sub>2</sub> particles. *J. Colloid Interface Sci.* 1997;188:387–395.
107. Sousa SR, Bras MM, Moradas-Ferreira P, Barbosa MA. Dynamics of fibronectin adsorption on TiO<sub>2</sub> surfaces. *Langmuir* 2007;23:7046–7054.
108. Aubin-Tam ME, Hamad-Schifferli K. Structure and function of nanoparticle–protein conjugates. *Biomed. Mater.* 2008;034001.
109. McClellan SJ, Franses EI. Exclusion of bovine serum albumin from the air/water interface by sodium myristate. *Colloids Surf. B* 2003;30:1–11.
110. Kang F, Singh J. Conformational stability of a model protein (bovine serum albumin) during primary emulsification process of PLGA microspheres synthesis. *Int. J. Pharm.* 2003;260:149–156.
111. Aleksic M, Pease CK, Basketter DA, Panico M, Morris HR, Dell A. Investigating protein haptenation mechanisms of skin sensitizers using human serum albumin as a model protein. *Toxicol. In Vitro* 2007;21:723–733.
112. Boonsongrit Y, Abe H, Sato K, Naito M, Yoshimura M, Ichikawa H, et al. Controlled release of bovine serum albumin from hydroxyapatite microspheres for protein delivery system. *Mater. Sci. Eng. B* 2008;148:162–165.
113. Wehmeyer J, Bizios R, Garcia CD. Adsorption of BSA to nanostructured TiO<sub>2</sub>. 2008:submitted.
114. van der Veen M, Norde W, Stuart MC. Electrostatic interactions in protein adsorption probed by comparing lysozyme and succinylated lysozyme. *Colloids Surf. B Biointerfaces* 2004;35:33–40.
115. Haynes CA, Norde W. Globular proteins at solid/liquid interfaces. *Colloids Surf. B Biointerfaces* 1994;2:517–566.
116. D'Orazio P. Biosensors in clinical chemistry. *Clin. Chim. Acta* 2003;334:41–69.
117. Alaejos MS, Garcia Montelongo FJ. Application of amperometric biosensors to the determination of vitamins and alpha-amino acids. *Chem. Rev.* 2004;104:3239–3266.
118. Wang J. Electrochemical biosensors: towards point-of-care cancer diagnostics. *Biosens. Bioelectron.* 2006;21:1887–1892.
119. Rogers KR. Recent advances in biosensor techniques for environmental monitoring. *Anal. Chim. Acta* 2006;568:222–231.
120. Gooding JJ. Biosensor technology for detecting biological warfare agents: recent progress and future trends. *Anal. Chim. Acta* 2006;559:137–151.
121. Gómez-Hens A, Fernández-Romero JM, Aguilar-Caballeros MP. Nanostructures as analytical tools in bioassays. *Trends Anal. Chem.* 2008;27:394–406.
122. Cai C, Chen J. Direct electron transfer of glucose oxidase promoted by carbon nanotubes. *Anal. Biochem.* 2004;332:75–83.
123. Zhang M, Smith A, Gorski W. Carbon nanotube-chitosan system for electrochemical sensing based on dehydrogenase enzymes. *Anal. Chem.* 2004;76:5045–50.
124. Lenihan JS, Gavalas VG, Wang J, Andrews R, Bachas LG. Protein immobilization on carbon nanotubes through a molecular adapter. *J. Nanosci. Nanotechnol.* 2004;4:600–604.
125. Lin Y, Taylor S, Li H, Fernando KAS, Qu L, Wang W, et al. Advances toward bioapplications of carbon nanotubes. *J. Mater. Chem.* 2004;14:527–541.
126. Liu Y, Qu X, Guo H, Chen H, Liu B, Dong S. Facile preparation of amperometric laccase biosensor with multifunction based on the matrix of carbon nanotubes-chitosan composite. *Biosens. Bioelectron.* 2006;21:2195–2201.



127. Qi H, Zhang C, Li X. Amperometric third-generation hydrogen peroxide biosensor incorporating multiwall carbon nanotubes and hemoglobin. *Sens. Actuators B* 2006;114:364–370.
128. Weber J, Kumar A, Kumar A, Bhansali S. Novel lactate and pH biosensor for skin and sweat analysis based on single walled carbon nanotubes. *Sens. Actuators B* 2006;117:308–313.
129. Zhang M, Gorski W. Electrochemical sensing based on redox mediation at carbon nanotubes. *Anal. Chem.* 2005;77:3960–3965.
130. Sánchez S, Roldán M, Pérez S, Fàbregas E. Toward a fast, easy, and versatile immobilization of biomolecules into carbon nanotube/polysulfone-based biosensors for the detection of hCG hormone. *Anal. Chem.* 2008;80:6508–6514.
131. Eggins BR. Sensing elements. In: Eggins BR, (ed.) *Chemical Sensors and Biosensors*. West Sussex, England: Wiley; 2002. pp. 98–106.
132. Krajewska B. Application of chitin- and chitosan-based materials for enzyme immobilizations: a review. *Enzyme Microb. Technol.* 2004;35:126–139.
133. López MS-P, López-Cabarcos E, López-Ruiz B. Organic phase enzyme electrodes. *Biomol. Eng.* 2006;23:135–147.
134. Mizutani H, Miyahara I, Hirotsu K, Nishina Y, Shiga K, Setoyama C, et al. Three-dimensional structure of porcine kidney D-amino acid oxidase at 3.0 Å resolution. *J. Biochem.* 1996;120:14–17.
135. Yagi K, Ohishi N. Structure and function of D-amino acid oxidase – IV. Electrophoretic and ultracentrifugal approach to the monomer equilibrium. *J. Biochem.* 1972;71:993–998.
136. Tishkov VI, Khoronenkova SV. D-amino acid oxidase: structure, catalytic mechanism, and practical application. *Biochemistry* 2005;70:40–54.
137. Tessema M, Larsson T, Buttler T, Csoregi E, Ruzgas T, Nordling M, et al. Simultaneous amperometric determination of some mono-, di-, and oligosaccharides in flow injection and liquid chromatography using two working enzyme electrodes with different selectivity. *Anal. Chim. Acta* 1997;349:179–188.
138. Wang J, Chen G. Microchip capillary electrophoresis with electrochemical detector for fast measurements of aromatic amino acids. *Talanta* 2003;60:1239–1244.
139. Nagata Y, Akino T, Ohno K, Kataoka Y, Ueda T, Sakurai T, et al. Free D-amino acids in human plasma in relation to senescence and renal diseases. *Clin. Sci.* 1987;73:105–8.
140. D’Aniello A, D’Onofrio G, Pischetola M, D’Aniello G, Vetere A, Petrucelli L, et al. Biological role of D-amino acid oxidase and D-aspartate oxidase. Effects of D-amino acids. *J. Biol. Chem.* 1993;268:26941–26949.
141. Hall D, Gogos JA, Karayiorgou M. The contribution of three strong candidate schizophrenia susceptibility genes in demographically distinct populations. *Genes Brain Behav.* 2004;3:240–248.
142. Quan Z, Song Y, Feng Y, LeBlanc MH, Liu Y-M. Detection of D-serine in neural samples by saccharide enhanced chiral capillary electrophoresis. *Anal. Chim. Acta* 2005;528:101–106.
143. Hamase K, Morikawa A, Zaitu K. Amino acids in mammals and their diagnostic value. *J. Chromatogr. B* 2002;781:73–91.
144. Pilone MS, Pollegioni L. D-amino acid oxidase as an industrial biocatalyst. *Biocatal. Biotransform.* 2002;20:145–159.
145. Betancor L, Hidalgo A, Fernandez-Lorente G, Mateo C, Rodriguez V, Fuentes M, et al. Use of physicochemical tools to determine the choice of optimal enzyme: stabilization of D-amino acid oxidase. *Biotechnol. Prog.* 2003;19:784–748.
146. Fernandez-Lafuente R, Rodriguez V, Mateo C, Fernandez-Lorente G, Arminsen P, Sabuquillo P, et al. Stabilization of enzymes (-amino acid oxidase) against hydrogen peroxide via immobilization and post-immobilization techniques. *J. Mol. Catal., B Enzym.* 1999;7:173–179.
147. Duran N, Rosa MA, Annibale A, Gianfreda L. Applications of laccases and tyrosinases (phenoloxidases) immobilized on different supports: a review. *Enzyme Microb. Technol.* 2002;31:907–931.
148. Rivas GA, Rubianes MD, Rodríguez MC, Ferreyra NF, Luque GL, Pedano ML, et al. Carbon nanotubes for electrochemical biosensing. *Talanta* 2007;74:291–307.
149. Karajanagi SS, Vertegel AA, Kane RS, Dordick JS. Structure and function of enzymes adsorbed onto single-walled carbon nanotubes. *Langmuir* 2004;20:11594–11599.
150. Schulz B, Chan D, Bäckström J, Rübhausen M. Spectroscopic ellipsometry on biological materials – investigation of hydration dynamics and structural properties. *Thin Solid Films* 2004;455–456:731–734.
151. Danny C, Benjamin S, Kathrin G, Heike Hedwig M, Michael R. In vivo spectroscopic ellipsometry measurements on human skin. *J. Biomed. Opt.* 2007;12:014023.
152. Santos O, Kosoric J, Hector MP, Anderson P, Lindh L. Adsorption behavior of statherin and a statherin peptide onto hydroxyapatite and silica surfaces by in situ ellipsometry. *J. Colloid Interface Sci.* 2008;318:175–182.
153. Arwin H. Is ellipsometry suitable for sensor applications? *Sens. Actuators A* 2001;92:43–51.



154. Demirel G, Çağlayan MO, Garipcan B, Piskin E. A novel DNA biosensor based on ellipsometry. *Surf. Sci.* 2008;602:952–959.
155. Nabok A, Tsargorodskaya A, Davis F, Higson SPJ. The study of genomic DNA adsorption and subsequent interactions using total internal reflection ellipsometry. *Biosens. Bioelectron.* 2007;23:377–383.
156. Wenmackers S, Pop SD, Roodenko K, Vermeeren V, Williams OA, Daenen M, et al. Structural and optical properties of DNA layers covalently attached to diamond surfaces. *Langmuir* 2008;24:7269–7277.
157. Cristofolini L, Berzina T, Erokhin V, Tenti M, Fontana MP, Erokhina S, et al. The structure of DNA-containing complexes suggests the idea for a new adaptive sensor. *Colloids Surf. A* 2008;321:158–162.
158. Carlsson J, Winqvist F, Danielsson B, Lundström I. Biosensor discrimination of meat juice from various animals using a lectin panel and ellipsometry. *Anal. Chim. Acta* 2005;547:229–236.
159. Jin G, Tengvall P, Lundström I, Arwin H. A biosensor concept based on imaging ellipsometry for visualization of biomolecular interactions. *Anal. Biochem.* 1995;232:69–72.
160. van Noort D, Rumberg J, Jager EWH, Mandenius CF. Silicon based affinity biochips viewed with imaging ellipsometry. *Meas. Sci. Technol.* 2000;11:801–808.
161. Bae YM, Oh B-K, Lee W, Lee WH, Choi J-W. Immunosensor for detection of *Legionella pneumophila* based on imaging ellipsometry. *Mater. Sci. Eng. C* 2004;24:61–64.
162. Bae YM, Park K-W, Oh B-K, Lee WH, Choi J-W. Immunosensor for detection of *Salmonella typhimurium* based on imaging ellipsometry. *Colloids Surf. A* 2005;257–258:19–23.
163. Bae YM, Oh BK, Lee W, Lee WH, Choi JW. Immunosensor for detection of *Yersinia enterocolitica* based on imaging ellipsometry. *Anal. Chem.* 2004;76:1799–1803.
164. Marinkova D, Bivolarska M, Ahtapodov L, Yotova L, Mateva R, Velinov T. Plasmon microscopy and imaging ellipsometry of *Artrobacter oxydans* attached on polymer films. *Colloids Surf. A* 2008;65:276–280.
165. Pereira EMA, Sierakowski MR, Jó TA, Moreira RA, Monteiro-Moreira ACO, França RFO, et al. Lectins and/or xyloglucans/alginate layers as supports for immobilization of dengue virus particles. *Colloids Surf. B* 2008;66:45–52.
166. Wang Z, Jin G. Feasibility of protein A for the oriented immobilization of immunoglobulin on silicon surface for a biosensor with imaging ellipsometry. *J. Biochem. Biophys. Methods* 2003;57:203–211.
167. Qi C, Duan J-Z, Wang Z-H, Chen Y-Y, Zhang P-H, Zhan L, et al. Investigation of interaction between two neutralizing monoclonal antibodies and SARS virus using biosensor based on imaging ellipsometry. *Biomed. Microdevices* 2006;8:247–253.
168. Wang Z-H, Jin G. Silicon surface modification with a mixed silanes layer to immobilize proteins for biosensor with imaging ellipsometry. *Colloids Surf. B* 2004;34:173–177.
169. Schuy S, Faiss S, Yoder NC, Kalsani V, Kumar K, Janshoff A, et al. Structure and Thermotropic phase Behavior of Fluorinated Phospholipid Bilayers: A combined Attenuated Total Reflection FTIR Spectroscopy and Imaging Ellipsometry Study. *J. Phys. Chem. B Biointerfaces* 2008;112:8250–8256.
170. Srivatsa V, Neil B, Yanming Z, Russell C. Evanescent-imaging-ellipsometry-based microarray reader. *J. Biomed. Opt.* 2006;11:014028.
171. Beyerlein D, Kratzmüller T, Eichhorn KJ. Study of novel polymer architectures on solid surfaces by variable angle spectroscopic and imaging ellipsometry. *Vib. Spectrosc* 2002;29:223–227.

Biological Interactions on Materials Surfaces  
Understanding and Controlling Protein, Cell, and Tissue  
Responses

Puleo, D.A.; Bizios, R. (Eds.)

2009, XX, 429 p., Hardcover

ISBN: 978-0-387-98160-4